

Hubble Space Telescope ultraviolet spectroscopy of blazars: emission lines properties and black hole masses

E. Pian, R. Falomo, A. Treves

Outline

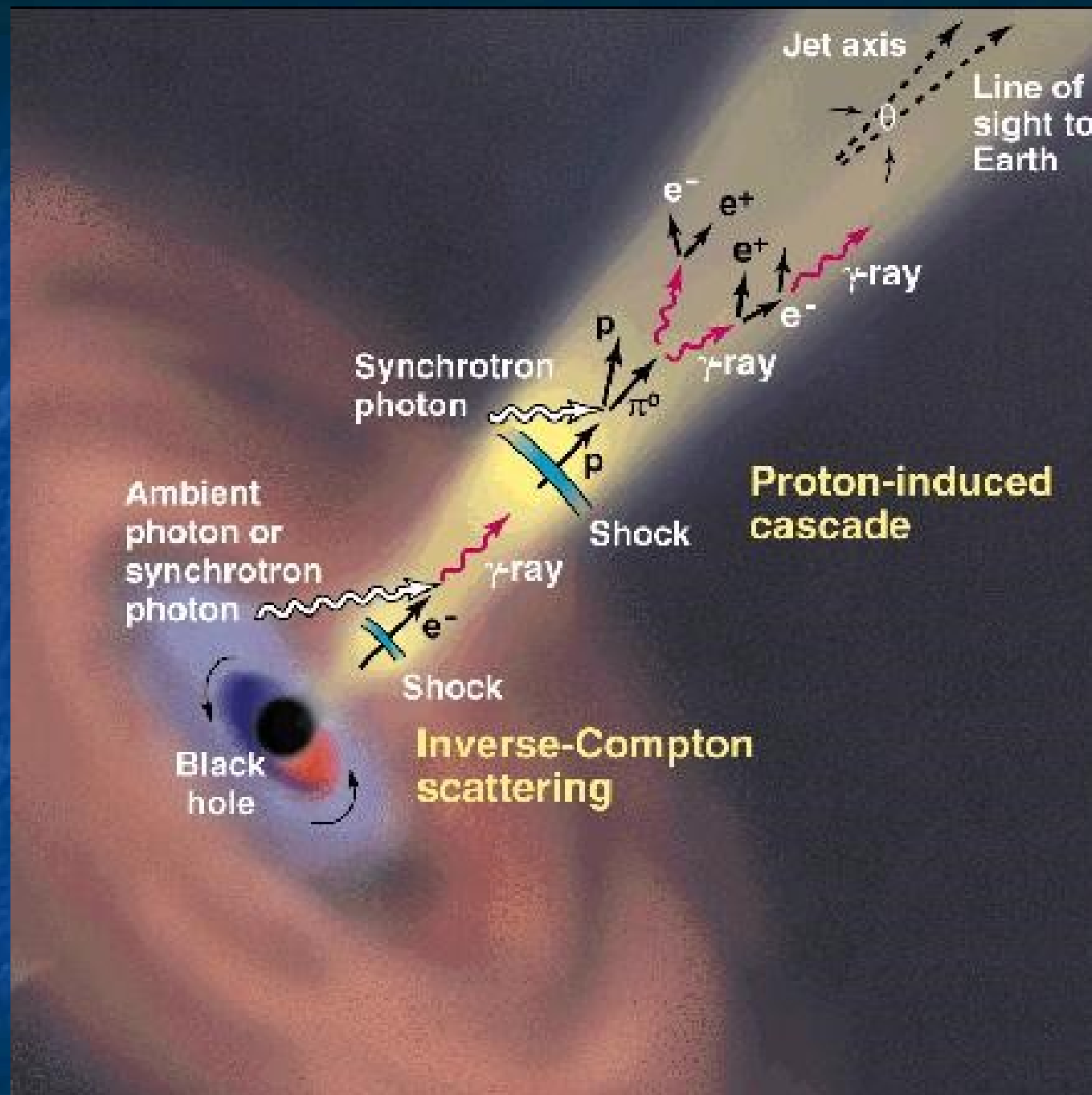
- Extra Background
- Introduction
- Sample Selection
- Data Analysis
- Results
 - Emission Line Properties
 - Black Hole Masses
 - Size of the BLR
 - Mass Estimates
- Conclusions



<http://www.clayharrison.com/truck/mytrucks-72ChevBlazer.html>

Extra Background

- Active Galactic Nuclei
- Quasi-Stellar Objects
 - Quasars
 - Radio Loud Quasars
 - Blazars
 - Highly Polarized Quasars
 - BL Lacertae Objects
 - PG Quasars
 - Seyfert Galaxies



Introduction

- Some blazars have broad emission lines superimposed on their optical and UV continua:
 - **Highly Polarized Quasars (HPQ)**, also know as Flat Spectrum Radio Quasars
 - *A few* **BL Lacertae objects**
 - Note that the emission lines of most BL Lac objects are generally overpowered by their continua.
- These emission lines indicate the energetics of blazars.
 - Some models predict that the **broad line region (BLR)** photons are upscattered to X-ray and gamma-ray energies by relativistic jet particles. The resulting high energy spectral component often dominates the total blazar output.

Introduction

- Specifically, the BLR may help determine the interplay between the accretion disk and the relativistic jet.
 - The relativist jets of blazars are more prominent than those in other **quasi-stellar objects (QSO)** and **Seyferts**.
- Also, the broad emission lines of **active galactic nuclei (AGN)** can be used to estimate the mass of the central compact object - generally assumed to be a massive **black hole (BH)**.
 - Based on the dynamical effect of the BH on the nearby line-emitting gas clouds (i.e. Virial Theorem).
 - However, the Virial Theorem requires that the size of the BLR be known.
 - Done indirectly using optical or UV emission lines.
 - UV corresponds to a higher ionization state, and therefore probably originated closer to the central BH.

Introduction

- In this work, Pian et. al. study the UV emission lines of 16 blazars.
 - Observed by the **Hubble Space Telescope (HST)** and the **Faint Object Spectrograph (FOS)**.
 - Based on the radiative and kinematic properties of the BLR, they determine:
 - The luminosity of the BLR
 - The size of the BLR
 - The mass of the central BH
- Throughout this work, it is assumed:
 - $\Omega_m = 0.3$
 - $\Omega_\Lambda = 0.7$
 - $H_0 = 72 \text{ km/s/Mpc}$

Sample Selection

- Used the HST archive at <http://archive.stsci.edu> as the source for their FOS blazar spectra.
- Includes both pre- and post- **Corrective Optics Space Telescope Axial Replacement (COSTAR)** observations.
- Also included PKS 1229-021 and **3C 273**
 - PKS 1229-021 has low polarization, but significant emission in the MeV-GeV range.
 - 3C 273 has properties between blazars and Seyfert galaxies.
- Selected spectra taken with high-resolution UV gratings:
 - G130H, G190H, G270H, G400H

Sample Selection

- Total of 24 objects with measurable spectra
 - Spectra taken with the same grating within one day were averaged to increase the signal-to-noise.
- 16 objects had 3σ emission line detections
 - 6 of these sources also had low-resolution (G160L) spectra available within one day, but are neglected.

Table 1. Parameters of Blazars observed with HST FOS

Object	Alt. Name	z	E_{B-V}^a	Date	Range ^b	α_λ^c	f_{1350}^d
BL0403-1316		0.571	0.058	11.4 Oct 1991	1570-4780	1.20 ± 0.04	1.98
BL0420-0127		0.915	0.125	23.5 Dec 1996	2220-3280	0.00 ± 0.22	0.80
BL0537-4406		0.896	0.037	16.7 Sep 1993	2220-3280	0.07 ± 0.20	1.64
BL0637-7513		0.656	0.095	25.6 May 1992	1610-3270	1.25 ± 0.06	5.64
BL0954+5537	4C 55.17	0.901	0.0088	20.9 Jan 1993	1570-3280	0.31 ± 0.08	0.60
BL1144-3755		1.048	0.097	15.6 Jul 1993	2220-3280	0.20 ± 0.23	1.42
BL1156+2931		0.729	0.019	26.7 Feb 1995	1620-4780	0.52 ± 0.04	8.29
BL1226+0219	3C 273	0.158	0.02	16.8 Jan 1991	1090-3280	1.68 ± 0.04	245
				09.4 Jul 1991	1290-3290	1.35 ± 0.06	117
BL1229-0207		1.045	0.032	01.1 Jan 1995	1570-3280	0.81 ± 0.12	2.58
BL1253-0531	3C 279	0.538	0.028	08.5 Apr 1992	1570-4780	0.18 ± 0.03	1.54
BL1611+3420	DA 406	1.401	0.018	04.9 Apr 1992	2220-4780	0.91 ± 0.08	0.81
BL1641+3954	3C 345	0.595	0.013	07.9 Jun 1992	1600-4770	0.65 ± 0.04	3.03
				20.4 Aug 1995	1570-4800	0.96 ± 0.16	0.43
BL2223-0512	3C 446	1.404	0.075	11.8 Sep 1991	2220-4780	0.00 ± 0.11	0.35
BL2230+1128	CTA 102	1.037	0.072	12.1 Sep 1991	2220-4780	1.13 ± 0.06	1.95
BL2243-1222		0.63	0.051	09.4 Oct 1993	1610-3270	1.59 ± 0.07	5.18
BL2251+1552	3C 454.3	0.859	0.105	11.9 Sep 1991	1620-4770	0.90 ± 0.04	2.86
				15.3 Nov 1991	1620-3270	0.51 ± 0.10	4.35
				19.4 Aug 1995	1700-4800	1.08 ± 0.09	1.72

^a From the maps of Schlegel et al. (1998).

^b Observed wavelength range, in Å.

^c Spectral index of the power-law fitted to the dereddened spectra ($f_\lambda \propto \lambda^{-\alpha}$).

^d Normalization of the dereddened power-law continuum at 1350 Å (rest frame), in $10^{-15} \text{ erg s}^{-1} \text{ cm}^{-2} \text{ Å}^{-1}$.

Data Analysis

- Applied the following corrections:
 - The Galactic absorption using the maps of Schlegel, Finkbeiner, and Davis (1998).
 - The extinction curve of Cardelli, Clayton, and Mathis (1989).
- By fitting a linear local continuum on either side of the emission lines, they measured:
 - Equivalent widths (EWs)
 - The EW uncertainties are given by 2σ variation of the local continuum.
 - Full width at half maximum (FWHM)
 - Intensity

Data Analysis

- For each object:
 - Combine spectra taken within one day (using different gratings)
 - Exclude regions that include emission or absorption features
 - Bin the signal into 20-50 Å intervals.
 - Fit the continuum with a power law
 - In addition to the statistical errors, add a 5% systematic error to account for calibration uncertainties

Table 2: Emission Lines Measurements

Object	z	$\text{Ly}\beta^a$		$\text{Ly}\alpha^a$		Si IV		C IV		C III		Mg II	
		EW ^b	FWHM ^b	EW	FWHM	EW	FWHM	EW	FWHM	EW	FWHM	EW	FWHM
BL0403-1316	0.571	–	–	135 ± 4	14	9.8 ± 0.7	22	128 ± 4	17	26 ± 1	18	33 ± 3	30
BL0420-0127	0.915	–	–	105 ± 6	11	7.2 ± 0.8	19	56 ± 2	17	–	–	–	–
BL0537-4406	0.896	–	–	20 ± 2	12	1.7 ± 0.4	13	11.4 ± 0.7	11	–	–	–	–
BL0637-7513	0.656	11 ± 2	15	89 ± 2	11	4.5 ± 1	19	43 ± 2	11	12 ± 1	13	–	–
BL0954+5537	0.901	–	–	40 ± 1	11 ^c	–	–	25 ± 1	12 ^c	–	–	–	–
BL1144-3755	1.048	–	–	4.1 ± 0.6	14	–	–	4.6 ± 0.8	14	–	–	–	–
BL1156+2931	0.729	–	–	12.0 ± 0.8	18	1.1 ± 0.3	20	8.5 ± 0.5	26	–	–	–	–
BL1226+0219 ^d	0.158	2.6 ± 0.5	15	52 ± 2	12	–	–	26.8 ± 0.9	18	8.8 ± 0.3	19	6.6 ± 0.5	24
BL1226+0219 ^e	0.158	–	–	43 ± 3	14	–	–	31 ± 2	19	9.1 ± 0.6	24	8.5 ± 0.6	25
BL1229-0207	1.045	12 ± 1	13	94 ± 4	13	5.7 ± 0.5	25	42 ± 2	19	–	–	–	–
BL1253-0531	0.538	–	–	22 ± 1	13	–	–	20 ± 1	20 ^c	3.9 ± 0.5	15	6.4 ± 0.5	24
BL1611+3420	1.401	18 ± 2	26	58 ± 2	14	6.3 ± 0.9	27	48 ± 2	24	7 ± 1	34	–	–
BL1641+3954 ^f	0.595	–	–	67 ± 3	15	6 ± 1	20	71 ± 3	24	14.8 ± 0.9	21	22 ± 1	39
BL1641+3954 ^g	0.595	–	–	149 ± 36	14	16 ± 5	28	150 ± 16	22	45 ± 8	27	91 ± 19	25
BL2223-0512	1.404	23 ± 2	15	120 ± 3	10	–	–	58 ± 5	19	14 ± 3	40	–	–
BL2230+1128	1.037	–	–	77 ± 2	13	2.9 ± 0.4	19	29 ± 1	15	10.8 ± 0.6	21	–	–
BL2243-1222	0.63	16 ± 2	13	102 ± 2	10	8.5 ± 0.7	19	55 ± 1	12	13.3 ± 0.6	13	–	–
BL2251+1552 ^h	0.859	15 ± 1	12	89 ± 2	11	3.2 ± 0.5	25	31.8 ± 0.8	16	13.4 ± 0.7	24	–	–
BL2251+1552 ⁱ	0.859	8.3 ± 0.7	11	50 ± 1	14	–	–	16.8 ± 0.4	14	–	–	–	–
BL2251+1552 ^j	0.859	–	–	74 ± 7	11	–	–	36 ± 3	18	12 ± 2	18	–	–

^a The $\text{Ly}\alpha$ and $\text{Ly}\beta$ line EW measurements may have a residual contamination by the N V $\lambda 1240$ and O VI $\lambda 1034$ lines, respectively. This possible contamination does not exceed $\sim 10\%$. We have deblended the contamination in the FWHM measurements.

^b At rest frame, in Å. Uncertainties on the FWHM values are about 15%.

^c This line has an asymmetric profile, with a more prominent red wing.

^d 16.8 Jan 1991.

^e 9.4 Jul 1991.

^f 7.9 Jun 1992.

^g 20.4 Aug 1995.

^h 11.9 Sep 1991.

ⁱ 15.3 Nov 1991.

^j 19.4 Aug 1995.

Results

- The observed blazars fall between $z=0.158$ and $z=1.404$, with $\langle z \rangle = 0.84 \pm 0.31$
- The major detected lines are:
 - Ly β , Ly α , C IV $\lambda 1549$, C III $\lambda 1909$, Si IV $\lambda 1400$, and sometimes Mg II $\lambda 2798$
- In 3 cases, multiple epoch of observation are available:
 - 3C 273, 3C 345, 3C 454.3
 - Observed variations in line and continuum emission over a factor of 2 and 7, respectively.
 - However, there are too few observations to correlate line and continuum variability.

Emission Line Properties

- All UV spectra were averaged together to maximize the signal-to-noise ratio.
- Composite spectrum is similar to normal QSOs
- Also has a similar line ratio compared to other AGNs

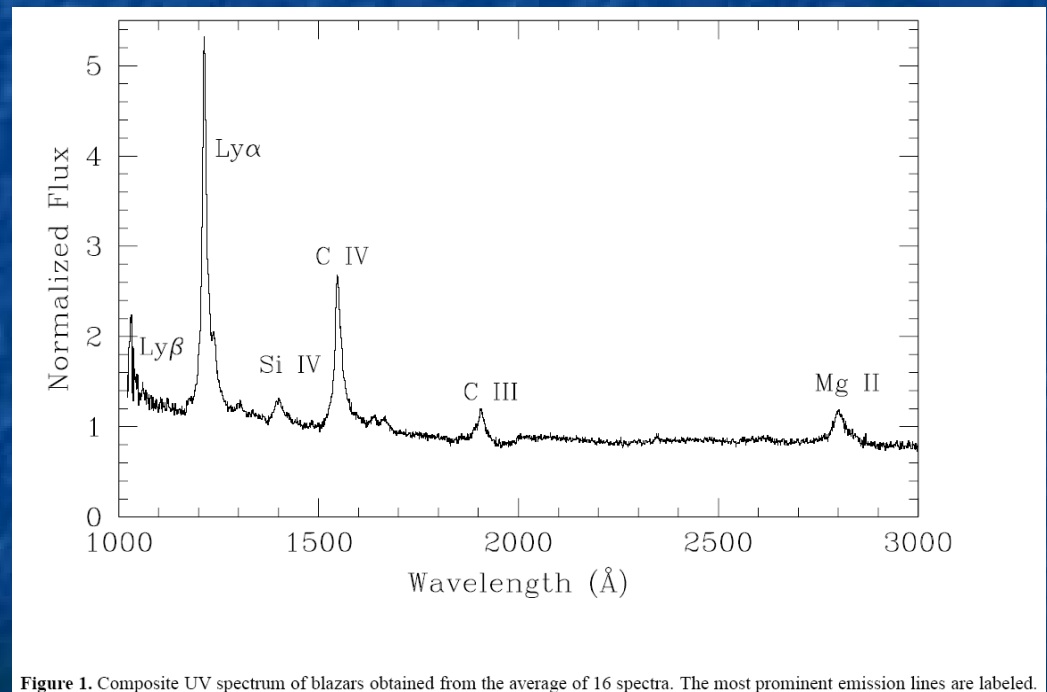


Figure 1. Composite UV spectrum of blazars obtained from the average of 16 spectra. The most prominent emission lines are labeled.

Pian et. al. 2005

- Intensity ratio of Ly α versus C IV λ 1549 for blazars is consistent with that of other **radio loud quasars (RLQs)**.

- Likewise for other intensity ratios

- Implies that the BLR in blazars and RLQs have similar structures

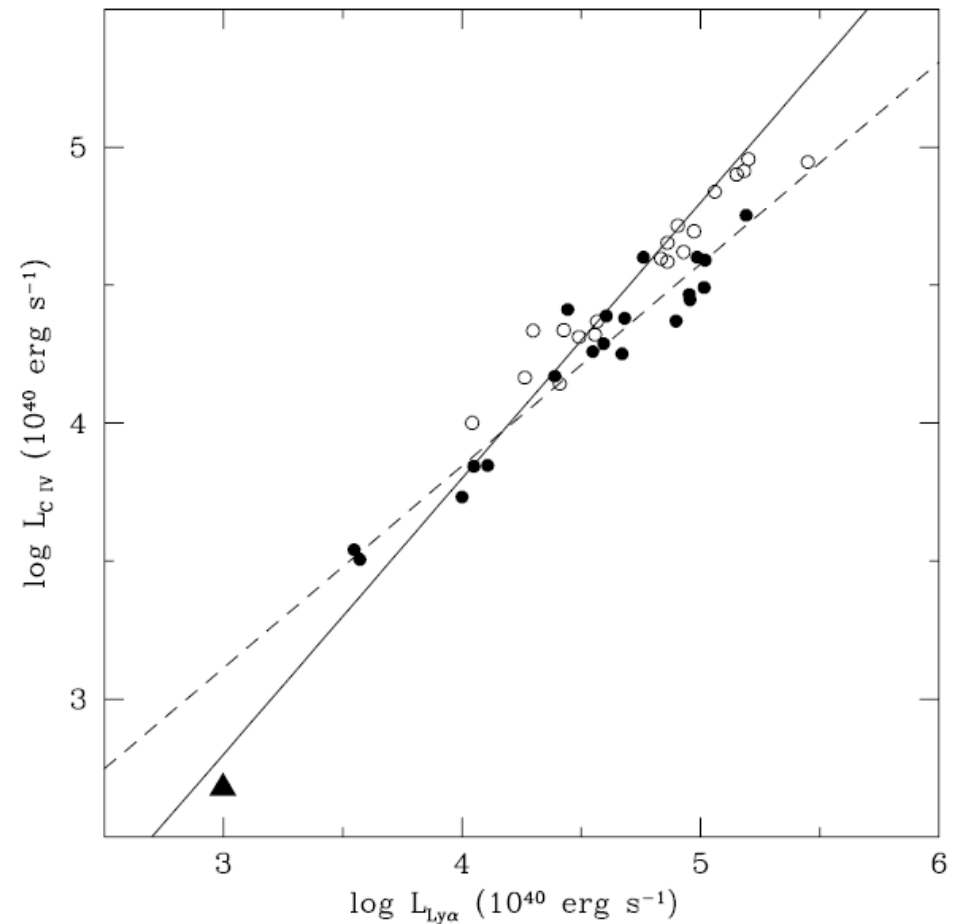


Figure 2. Luminosities of C IV λ 1549 and Ly α emission lines for the blazars in our list (filled circles). Line measurements of a given source at multiple epochs have not been averaged. The Ly α and C IV λ 1549 emission line intensities have been normalized to their respective average values. The solid line is the expected C IV λ 1549 to Ly α intensity ratio ($L(\text{C IV } \lambda 1549) = 0.63 \times L(\text{Ly}\alpha)$, e.g. Francis et al. 1991). The dashed line is the least square regression line $L(\text{C IV } \lambda 1549) = 8.3 \times L(\text{Ly}\alpha)^{0.73}$. For comparison, the line luminosities of 19 RLQ (open circles) from Wills et al. (1995) and of 3C 390 (triangle) are also shown.

Emission Line Properties

Table 3. Composite ultraviolet blazar spectrum.

Line	EW ^a	FWHM ^a	Rel. Intensity ^b	Ratio ^c	Ratio (LBQS) ^d	Ratio (RLQa) ^e	Ratio (RLQb) ^f
Ly β	6.5 \pm 0.5	10	8.9 \pm 0.5	10.6	9.3	19	19.1
Ly α	71 \pm 3	22	84 \pm 3	100	100	100	100
SiIV	5.2 \pm 0.7	21	5.6 \pm 0.7	6.6	19	6.8	8.6
C IV	45 \pm 2	20	45 \pm 1	53	63	66	52
C III]	7 \pm 1	23	6.6 \pm 0.7	7.8	29	11	13.2
Mg II	19 \pm 2	30	16 \pm 1	19	34	24	22.3

^a At rest frame, in Å. Uncertainties are about \sim 15%.

^b Obtained from EW and continuum normalized to the flux at 1500 Å (rest frame).

^c Average percentage intensity ratio with respect to Ly α as resulting from our measurements.

^d Same as in Col. 5 for 718 objects in the Large Bright Quasar Survey (Francis et al. 1991).

^e Same as in Col. 5 for 60 radio loud quasars (Zheng et al. 1997).

^f Same as in Col. 5 for 107 radio loud quasars (Telfer et al. 2002).

- Blazars:
 $\langle \log L(\text{Ly}\alpha) \rangle = 44.55 \pm 0.11$
- RLQ:
 $\langle \log L(\text{Ly}\alpha) \rangle = 44.72 \pm 0.12$
- But due to relativistic beaming, blazars have stronger continua
 - (smaller EW)

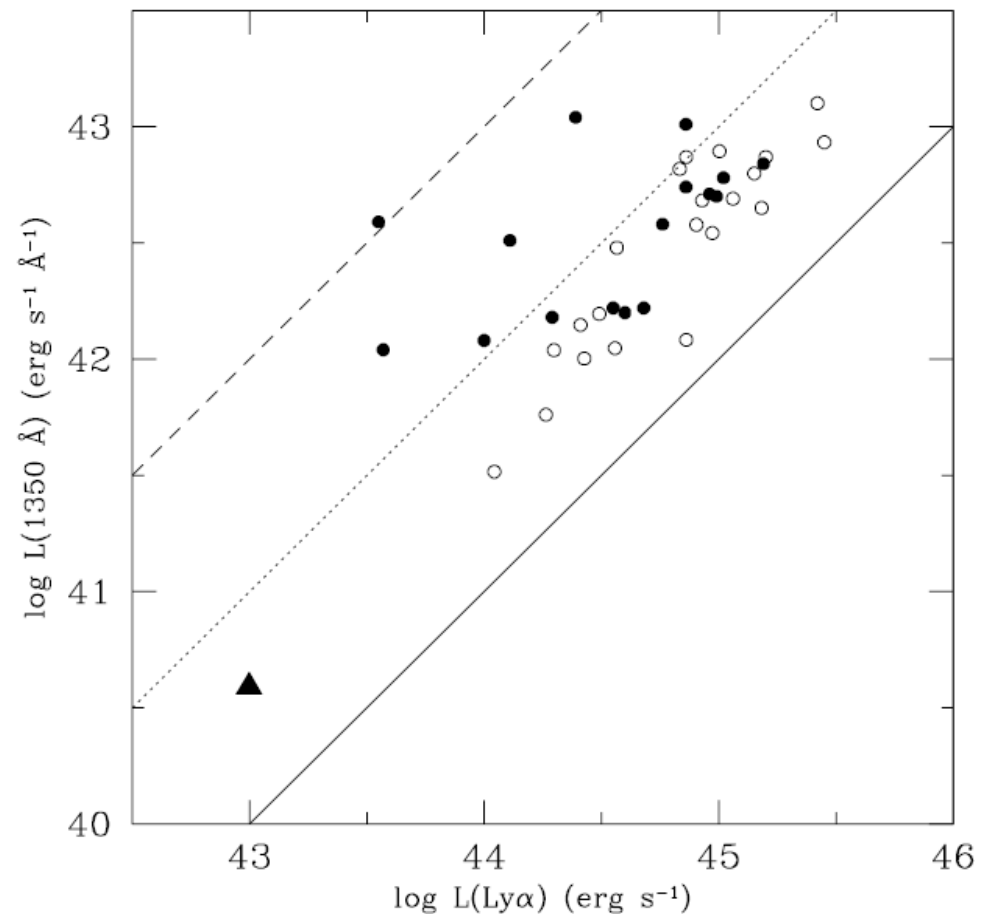


Figure 3. Ly α luminosity vs continuum luminosity at 1350 Å (rest frame) for blazars (filled circles) and RLQs (open circles). The triangle represents the low redshift RLQ 3C 390. The lines are the loci of the EW = 10 Å (dashed), 100 Å (dotted) and 1000 Å (solid).

Pian et. al. 2005

Emission Line Properties

- Non-thermal synchrotron radiation is subject to relativistic effects.
- Blazars are thought to be the same type of object as RLQs.
 - The relativistic jets of RLQs are directed away from our line of sight.
- Thus, the beaming amplification for our sample blazars can be found by assuming that their continuum luminosities are related to their Ly α luminosities in a similar manner to other RLQs.
 - Fitting a power law to the RLQ sample:

$$L(1350\text{\AA}) = 0.46 \times 10^{-3} L(\text{Ly}\alpha)^{1.02} \quad (1)$$

Black Hole Masses

- Assuming that the width of the broad emission lines are the result of the gravitational potential of a super massive BH:

$$M_{\text{BH}} = \frac{v^2 R_{\text{BLR}}}{G} \quad (2)$$

- v can be found from the FWHM, and depends on the geometry and kinematics of the BLR

Size of the BLR

- The most reliable method is the **reverberation mapping** technique of Peterson, Ferrarese, & Gilbert (2004).
- Uses the time lag between the emission and continuum light curves to determine the light crossing size of the BLR.
- Unfortunately, this method requires extensive monitoring of the source, and is thus only available for a few objects.
 - One of which is **BC 273**

Size of the BLR

- Alternatively, the size of the BLR can be found by using the empirical relationship with the continuum luminosity
- Derived using 15 **PG quasars** and 10 Seyfert galaxies having BLR radii given by the reverberation mapping technique
 - This sample includes **BC 273**, whose continuum luminosity was corrected for relativistic beaming by Eq. 1
 - Also, the variable continuum of the Seyfert, NGC 4151 was averaged at 1350\AA

- Fit with a power law:

$$R_{\text{BLR}} = (22.4 \pm 0.8) \left(\frac{\lambda L_{\lambda}(1350\text{\AA})}{10^{44} \text{ erg/s}} \right)^{0.61 \pm 0.02} \quad (3)$$

- If 3C 273 is excluded, the power-law index becomes 0.60 ± 0.02

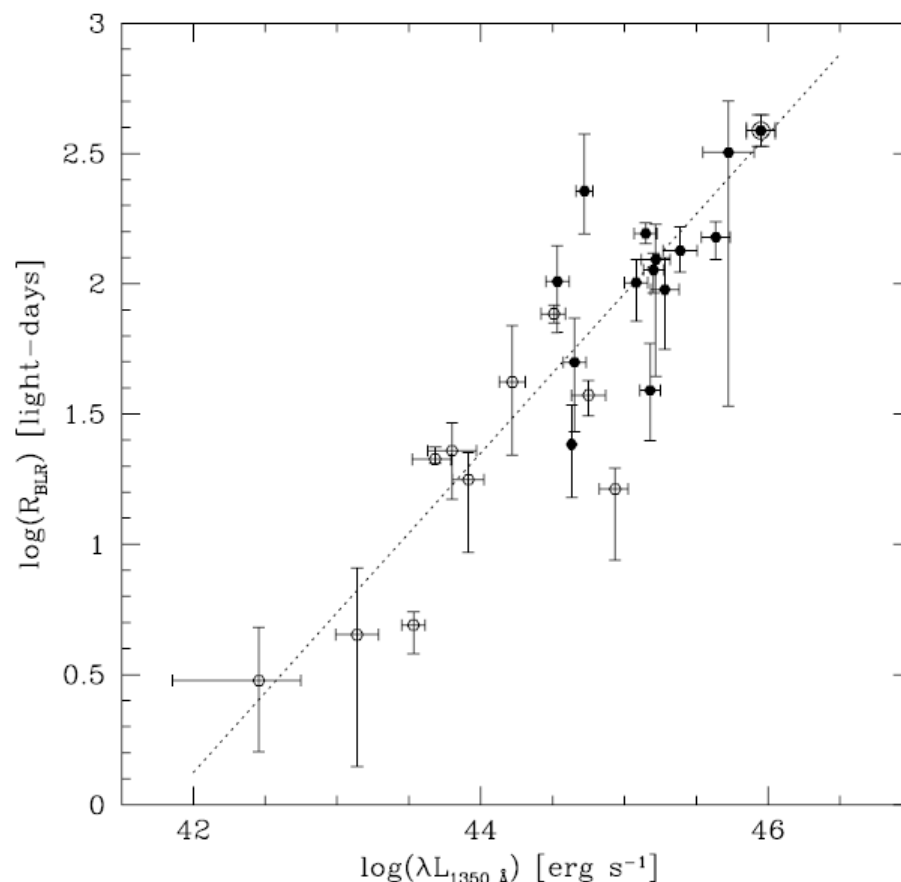


Figure 4. Size of the BLR as a function of the continuum power output at 1350 Å (rest frame) for the sample of PG quasars (filled circles) and Seyfert 1 galaxies (open circles) of Kaspi et al. (2000). The encircled point on the top right represents 3C 273. The luminosities have been taken from Vestergaard (2002). The line fitting the 2 quantities (Eq. 3) is also reported (dotted).

Size of the BLR

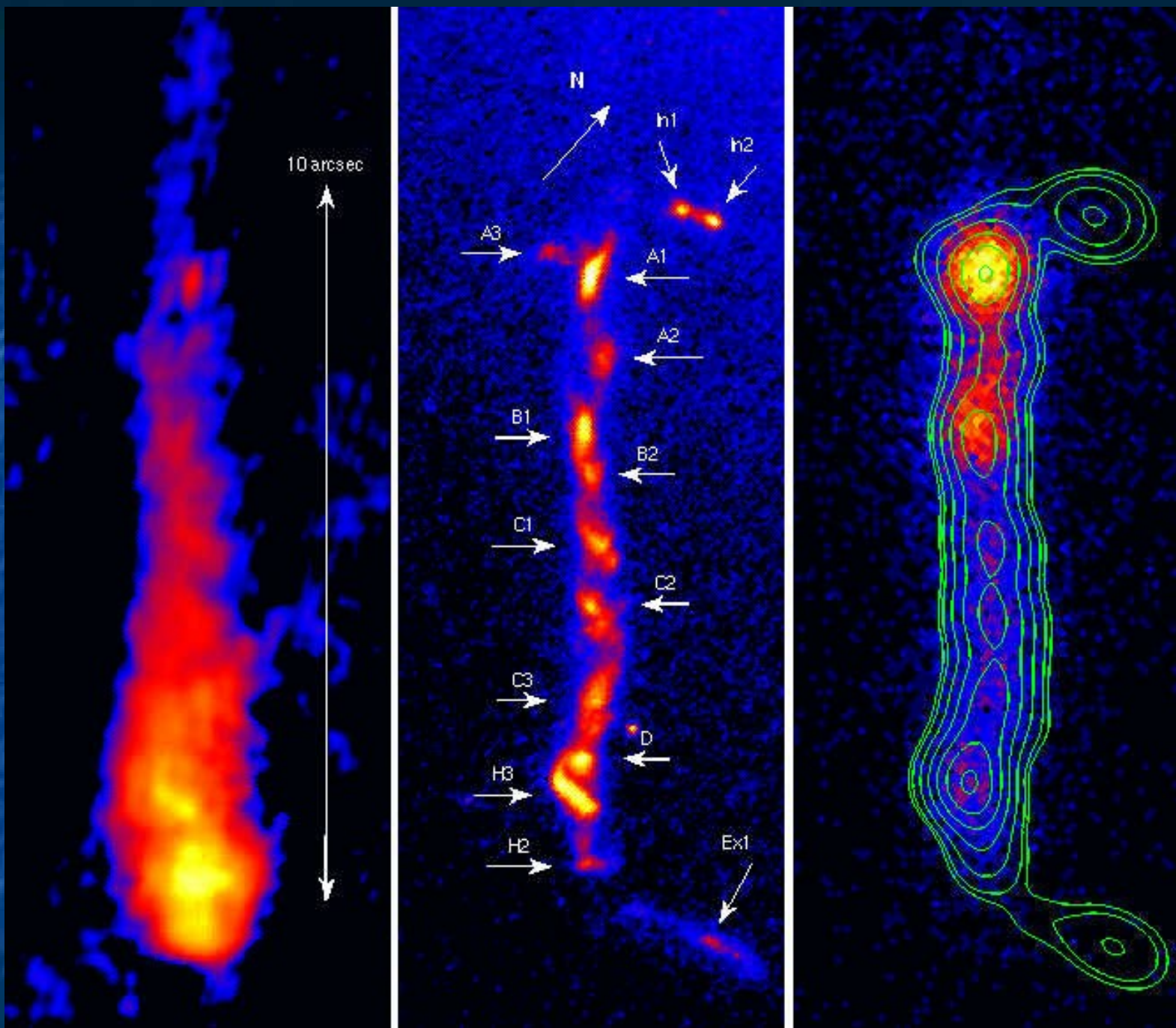
- Kapsi, Maoz, Netzer, Peterson, Vestergaard, & Jannuzi (2005) found 0.56 ± 0.05
- Kapsi, Smith, Netzer, Maoz, Jannuzi, and Giveon (2000) found 0.70 ± 0.03
 - In optical
- McLure and Jarvis (2002) found 0.50 ± 0.02
 - Based on a different sample of PQ quasars and Seyfert galaxies

Size of the BLR

- To apply this method to blazars, the UV continuum luminosity must be corrected for relativist beaming using Eq. 1:
 - $L(1350\text{\AA}) = 0.46 \times 10^{-3} L(\text{Ly}\alpha)^{1.02}$
- For 4 of our objects, this is a large correction (factor of ~ 3)
- Also note that for **3C 273**, the radius is consistent with that obtained by reverberation mapping.

Size of the BLR

- A third method of determining the BLR radius relates the luminosity of the BLR with the multi-wavelength spectrum of the blazar.
 - Only works for blazars, since other AGNs don't have spectra extending into the gamma-rays.
- 10 of our blazars have multi-wavelength spectra, and have been fit with inverse Compton and synchrotron radiation components.
 - Inverse Compton radiation dominates the x- and gamma-ray energies.
 - Includes scattering of relativistic electrons off of local photons and external radiation fields.



Martel et. al. 2003

Size of the BLR

- Using the fitted external photon density, U_{ext} and the observed BLR luminosities:

$$R_{\text{BLR}} = \sqrt{\frac{L_{\text{BLR}}}{4\pi c U_{\text{ext}} \delta}} \quad (4)$$

$$\delta = \frac{1}{\gamma(1 - \beta \cos \theta)}$$

Size of the BLR

- This **spectral energy distribution (SED)** method turns out to have “no clear correlation” with the BLR radii found by the other two methods.
- The radiation density of the BLR is generally less than the U_{ext} obtained via fitting the multi-wavelength spectra.
 - U_{ext} also incorrectly includes contributions from the accretion disk, other regions of the jet, etc.
 - Also, the uncertainties associated with the fit parameters are large.

Mass Estimates

- Combining Eq. 1 and 2, and assuming an isotropic distribution for the BLR:

$$M_{\text{BH}} = 3.26 \times 10^6 \left(\frac{\lambda L_{\lambda}(1350\text{\AA})}{10^{44} \text{ erg/s}} \right)^{0.61} \left(\frac{v_{\text{FWHM}}}{10^3 \text{ km/s}} \right)^2 M_{\text{Sun}} \quad (5)$$

Table 4. BLR Luminosities and Central Black Hole Masses.

Object	L_{BLR}^a	R_{BLR}^b	$R_{BLR,SED}^c$	M_{BH}^d	$M_{BH,LL}^e$	$M_{BH,WU}^f$	$M_{BH,W}^g$
BL0403-1316	22.6	145	...	2.4		12	
BL0420-0127	18.7	145	438	2.3	8	11	9
BL0537-4406	6.93	77	211	0.5	16		5
BL0637-7513	50.2	285	...	1.9		26	
BL0954+5537	5.38	66	312	0.5	8	1.2	
BL1144-3755	2.45	34	...	0.4			
BL1156+2931	13.7	115	158	4.3	8		
BL1226+0219	33.8	219	17	4.0	0.2		16
BL1229-0207	74.1	357	117	7.4	10		
BL1253-0531	2.42	36	104	0.8	4	2.7	3
BL1611+3420	34.1	196	92	6.2	40	37	
BL1641+3954	12.5	92	...	2.7		26	28
BL2223-0512	25.2	150	...	2.8			6
BL2230+1128	41.4	260	33	3.1	12.6		
BL2243-1222	47.8	271	...	2.1			
BL2251+1552	33.3	223	29	3.1	25	15	13

^a Luminosity of the BLR, in units of 10^{44} erg s⁻¹.

^b Size of the BLR computed via Eq. 3, in light days.

^c Size of the BLR computed using the SED method, (Eq. 4), in light days.

^d Mass of the central BH computed using Eq. 5, in units of $10^8 M_{\odot}$. The statistical uncertainties, dominated by the scatter of Eq. 3, are about a factor 2.

^e Mass of the central BH from Liang & Liu (2003).

^f Mass of the central BH from Woo & Urry (2002).

^g Mass of the central BH from Wang et al. (2004).

Pian et. al. 2005

- For blazars:
 $\langle \log M_{\text{BH}} \rangle = 8.31 \pm 0.10$
- For RLQ:
 $\langle \log M_{\text{BH}} \rangle = 8.41 \pm 0.08$
- There is no apparent correlation of BH mass with redshift.

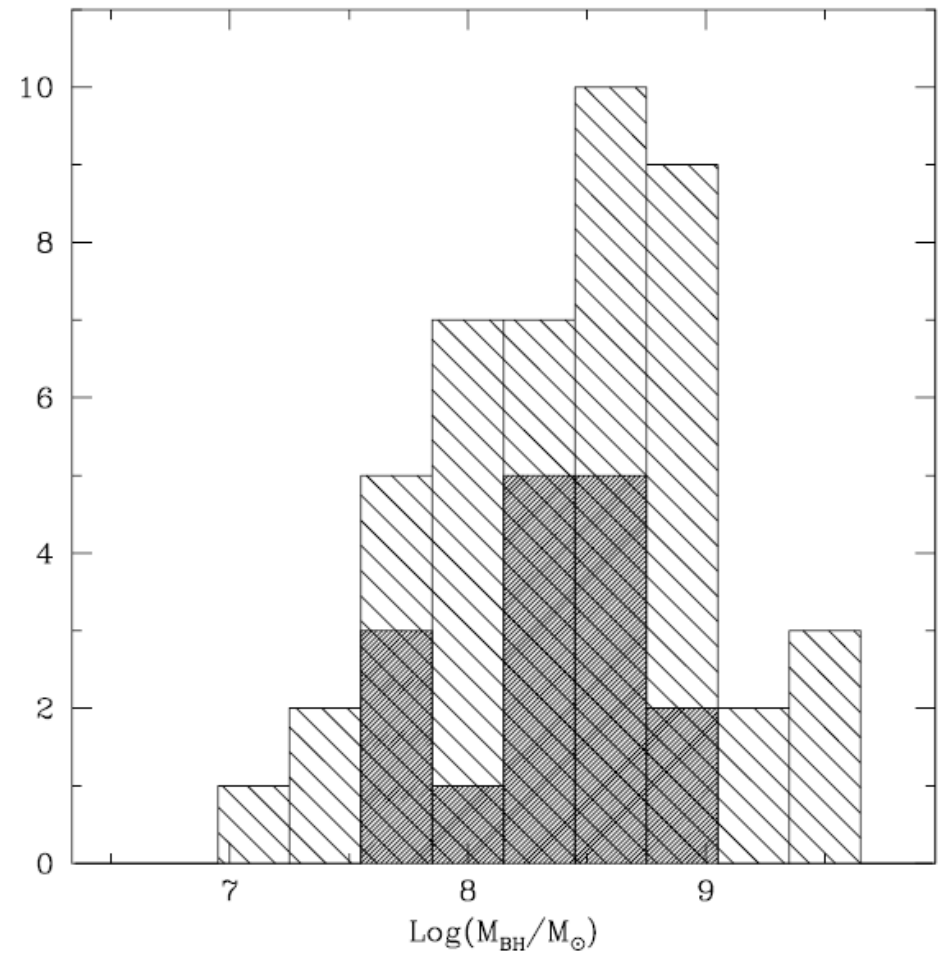


Figure 5. Histograms of central BH masses of AGNs. The simply hatched area represents the masses of PG quasars computed with Eq. 5 from the luminosities and C IV $\lambda 1549$ emission line FWHM values reported by Vestergaard (2002). The double-hatched area represents the BH masses of our blazar sample. Mass estimates obtained for a same source at different epochs have been averaged.

Conclusions

- The average blazar spectra is similar to that of RLQs.
- The size of the BLR for these blazars was determined by utilizing an empirical relationship with the luminosity in the UV.
 - These radii are consistent with those found in other studies.
- The SED method failed to produce consistent BLR radii.
- The average BH mass was found to be $2.8 \pm 2.0 \times 10^8 M_{\text{sun}}$ and are comparable to the masses found by other methods.
- The distribution of blazar BH masses is consistent with PG quasar masses.
 - This implies that the difference between radio-load and weak sources are not due to the BH mass, at least for ³³

References

- Pian, E., Falomo, R., & Treves, A. 2005, MNRAS, 361, 919
- S.A. Zeilik and M.Gregory, *Introductory Astronomy and Astrophysics*, (New York: Saunders College Publishing, 4th ed., 1998).
- http://www.astro.uni-wuerzburg.de/img/img_html/img_hochenergie_d.html
- http://hea-www.harvard.edu/XJET/source-d.cgi?3C_273
- http://imagine.gsfc.nasa.gov/docs/science/know_l2/active_galaxies.html
- <http://en.wikipedia.org/wiki/Blazar>